

THE LIMITS OF SISYPHUS COOLING

Y. Castin, J. Dalibard and C. Cohen-Tannoudji

Laboratoire de Spectroscopie Hertzienne de L'Ecole Normale Supérieure (*)
and Collège de France
24, Rue Lhomond, F-75231 Paris Cedex 05, France

Abstract: *We present a theoretical analysis of the Sisyphus cooling occurring in a 1-D polarization gradient molasses. Starting from the full quantum equations of motion, we show that, in the limit of large detunings, the steady state atomic density matrix depends only on a single parameter U_0/E_R , where U_0 is the depth of the optical potential wells and E_R the recoil energy. The minimal kinetic energy is found to be on the order of $40 E_R$ and is obtained for $U_0 \simeq 100 E_R$. We derive also simple analytical equations of motion which confirm the physical picture of Sisyphus cooling. Steady state solutions of these equations are obtained in the two limiting cases of jumping particles (optical pumping time τ_P shorter than the oscillation period $2\pi/\Omega_{osc}$ in an optical potential well) and oscillating particles ($\Omega_{osc}\tau_P \gg 1$).*

1. INTRODUCTION

Laser cooling is known to have led to extremely low atomic kinetic temperatures in the recent years [1]. Initially it was thought that Doppler cooling [2, 3] was sufficient to explain these temperatures. This type of laser cooling is based on the radiation pressure forces, exerted by identical counterpropagating laser waves on a moving atom, which become unbalanced because of opposite Doppler shifts. The temperatures achievable by Doppler cooling can be shown to be limited by the lower bound T_D :

$$k_B T_D = \hbar\Gamma/2. \quad (1.1)$$

However, the discovery in 1988 [4] of temperatures well below this theoretical Doppler limit T_D initiated a search for new cooling mechanisms, more effective than Doppler cooling.

First qualitative explanations were given soon after this experimental discovery [5, 6] and were followed by more quantitative treatments [7, 8]. They are based on the internal atomic ground state dynamics induced by the atomic motion in the polarization gradients of the molasses laser fields. These dynamics arise from the fact that the ground state of the atoms experimentally studied (Na, Cs) is degenerate. This had been left out of the previous theoretical models, which were dealing only with two level atoms. The internal atomic dynamics lead, for very low laser intensities, to long internal atomic pumping times which, when associated to differential light shifts of the various ground state sublevels, may be at the origin of a strong cooling and of sub Doppler temperatures.

In this paper, we restrict ourselves to 1D molasses. In such a case, two distinct cooling mechanisms in a laser polarization gradient can be identified [7]. The first one, on which we will focus

(*) Laboratoire associé au Centre National de la Recherche Scientifique et à l'Université Pierre et Marie Curie.

will focus in the following, occurs in the lin \perp lin configuration, formed by two orthogonally linearly polarized, counterpropagating plane waves. It arises from a ‘‘Sisyphus’’ effect: due to the spatial modulation of light shifts and optical pumping rates, the atom ‘‘ascends’’ more than it ‘‘descends’’ in its energy diagram. The second 1-D mechanism occurs in a superposition of two counterpropagating waves with σ_+ and σ_- polarizations. For a $J_g = 1 \longleftrightarrow J_e = 2$ atomic transition for instance, a strong cooling occurs, due to a differential scattering force induced by a very sensitive velocity-sensitive population difference appearing between the two ground state sublevels $|J_g, m_g = 1\rangle$ and $|J_g, m_g = -1\rangle$.

When the detuning $\delta = \omega_L - \omega_A$ between the laser and atomic frequencies is large compared to the natural width Γ , the Sisyphus mechanism leads, for very low velocities, to a cooling force and to a momentum diffusion coefficient stronger by a factor δ^2/Γ^2 than the ones for the second mechanism. We will therefore focus in the following on the Sisyphus cooling.

We will first (§ 2) give a qualitative description of Sisyphus cooling, restricting ourselves to a $J_g = 1/2 \longleftrightarrow J_e = 3/2$ transition. We will then present (§ 3) numerical results concerning the temperature achievable by this cooling. These results have been derived from a full quantum treatment of both internal and external degrees of freedom of the atom. Finally, we present in § 4 some elements for a semi-classical treatment of this process, in which the external motion can be analyzed in classical terms. We show that this approach allows some simple physical pictures, while giving results in good agreement with the exact quantum treatment.

2. QUALITATIVE DESCRIPTION OF SISYPHUS COOLING

2.1 The Laser Field

In this section, we outline the physical mechanism which leads to Sisyphus cooling for a $J_g = 1/2 \longleftrightarrow J_e = 3/2$ atomic transition (Fig. 1a). The laser electric field resulting from the superposition of two counterpropagating waves with respective polarizations ϵ_x and ϵ_y , respective phases at $z = 0$ equal to 0 and $-\pi/2$, and with the same amplitude \mathcal{E}_0 can be written:

$$\mathbf{E}(z, t) = \mathcal{E}^+(z)e^{-i\omega_L t} + c.c. \quad (2.1)$$

with :

$$\begin{aligned} \mathcal{E}^+(z) &= \mathcal{E}_0 (\epsilon_x e^{ikz} - i\epsilon_y e^{-ikz}) \\ &= \sqrt{2}\mathcal{E}_0 \left(\cos kz \frac{\epsilon_x - i\epsilon_y}{\sqrt{2}} + i \sin kz \frac{\epsilon_x + i\epsilon_y}{\sqrt{2}} \right). \end{aligned} \quad (2.2)$$

The total electric field is the superposition of two fields respectively σ_- and σ_+ polarized and with amplitudes $\mathcal{E}_0\sqrt{2}\cos kz$ and $\mathcal{E}_0\sqrt{2}\sin kz$. Therefore the resulting ellipticity depends on z . Light is circular (σ_-) at $z = 0$, linear along $(\epsilon_x - \epsilon_y)/\sqrt{2}$ at $z = \lambda/8\dots$ (Fig. 1b).

2.2 The Atomic Internal Dynamics

We now determine the positions of the light shifted energy levels, assuming here that the laser intensity is low, so that we can restrict our analysis to the ground state density matrix. Furthermore, since the laser polarization is a superposition of σ_+ and σ_- , and since $J_g < 1$, the optical excitation cannot create Zeeman coherences with $\Delta m = \pm 2$ in the ground state so that we can restrict our discussion to populations.

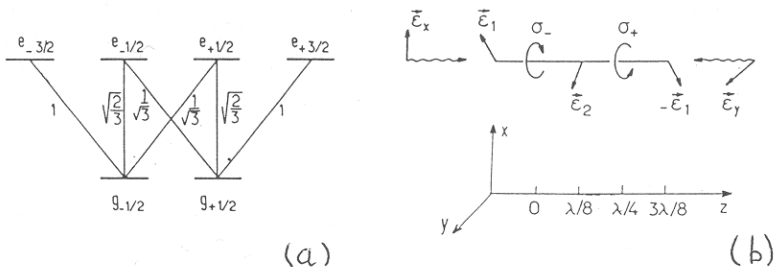


Fig.1a: Atomic level scheme and Clebsch-Gordan coefficients for a $J_g = 1/2 \leftrightarrow J_e = 3/2$ transition.

Fig.1b: The resulting polarization in a $\text{lin} \perp \text{lin}$ configuration.

Suppose, for example, that $z = 0$ so that the polarization is σ_- (Fig. 1b). The atom is optically pumped into $g_{-1/2}$ so that the steady-state populations of $g_{-1/2}$ and $g_{1/2}$ are equal to 1 and 0, respectively. We must also note that, since the σ_- transition starting from $g_{-1/2}$ is three times as intense as the σ_- transition starting from $g_{1/2}$, the light shift Δ'_- of $g_{-1/2}$ is three times larger (in modulus) than the light shift Δ'_+ of $g_{1/2}$. We assume here that, as usual in Doppler-cooling experiments, the detuning :

$$\delta = \omega_L - \omega_A \quad (2.3)$$

between the laser frequency ω_L and the atomic frequency ω_A is negative so that both light shifts are negative.

If the atom is at $z = \lambda/4$, where the polarization is σ_+ (Fig. 1b), the previous conclusions are reversed. The populations of $g_{-1/2}$ and $g_{1/2}$ are equal to 0 and 1, respectively, because the atom is now optically pumped into $g_{1/2}$. Both light shifts are still negative, but we now have $\Delta'_+ = 3\Delta'_-$.

Finally, if the atom is in a place where the polarization is linear, for example, if $z = \lambda/8, 3\lambda/8, \dots$, symmetry considerations show that both sublevels are equally populated and undergo the same (negative) light shift equal to $2/3$ times the maximum light shift occurring for a σ_+ or σ_- polarization.

All these results are summarized in Fig. 2a which shows as a function of z the light shifted energies of the two ground-state sublevels. The analytic expression for these light shifted energies $\hbar\Delta_{\pm}(z)$ can be derived simply from the expression for the laser field (2.2) and from the intensity factors of the various σ_+ and σ_- transitions given in Fig. 1a. One can indeed add independently the two light shifts created by the two σ_+ and σ_- standing waves appearing in (2.2), since $g_{1/2}$ and $g_{-1/2}$ are not connected to the same excited level :

$$\hbar\Delta_+(z) = \hbar\delta s_0 \sin^2 kz + \frac{1}{3}\hbar\delta s_0 \cos^2 kz = -U_0 + \frac{U_0}{2} \cos 2kz = -\frac{3U_0}{2} + U_+(z) \quad (2.4a)$$

$$\hbar\Delta_-(z) = \hbar\delta s_0 \cos^2 kz + \frac{1}{3}\hbar\delta s_0 \sin^2 kz = -U_0 - \frac{U_0}{2} \cos 2kz = -\frac{3U_0}{2} + U_-(z) \quad (2.4b)$$

with:

$$U_+(z) = U_0 \cos^2 kz \quad (2.4c)$$

$$U_-(z) = U_0 \sin^2 kz. \quad (2.4d)$$

The saturation parameter s_0 is defined as :

$$s_0 = \frac{\Omega^2/2}{\delta^2 + \Gamma^2/4}, \quad (2.5)$$

where Ω is the Rabi frequency for each of the two running waves, calculated for a Clebsh-Gordan coefficient equal to 1 and for a reduced dipole moment for the transition equal to d :

$$\Omega = -2d\mathcal{E}_0/\hbar. \quad (2.6)$$

The energy U_0 introduced in (2.4) :

$$U_0 = \frac{2}{3}\hbar(-\delta)s_0 > 0 \quad (2.7)$$

represents the modulation depth of the oscillating light shifted ground state sublevels. In the same way, one can derive the expression of the rate γ_+ at which the atom jumps from $g_{1/2}$ to $g_{-1/2}$:

$$\gamma_+ = \left(\frac{1}{3}\Gamma s_0 \cos^2 kz \right) \frac{2}{3} = \frac{2}{9}\Gamma s_0 \cos^2 kz. \quad (2.8)$$

This is the probability per unit time of absorbing a σ_- photon from $g_{1/2}$, and then decaying from $e_{-1/2}$ to $g_{-1/2}$ by emitting a π photon. In the same way, one gets :

$$\gamma_- = \frac{2}{9}\Gamma s_0 \sin^2 kz. \quad (2.9)$$

The characteristic internal relaxation time τ_p (*i.e.* optical pumping time) is then given by:

$$\frac{1}{\tau_p} = \gamma_+ + \gamma_- = \frac{2\gamma s_0}{9}. \quad (2.11)$$

2.3 Sisyphus Effect for a Moving Atom

We now consider an atom moving along Oz in the bi-potential $U_{\pm}(z)$. We suppose for instance that the atom is initially in the state $g_{1/2}$ with a kinetic energy much larger than the modulation depth U_0 (Fig. 2b). As the atom moves in $U_+(z)$, it may undergo a transition to $g_{-1/2}$. The rate γ_+ at which such a transition occurs is maximal around the tops of $U_+(z)$, the atom being then put in a valley for $U_-(z)$. This transition decreases the potential energy of the atom, while leaving its kinetic energy unchanged, if one neglects the momentum of the fluorescence photon involved in the process. From $g_{-1/2}$ the same sequence can be repeated so that the atom on the average climbs more than it goes down in its energy diagram. An

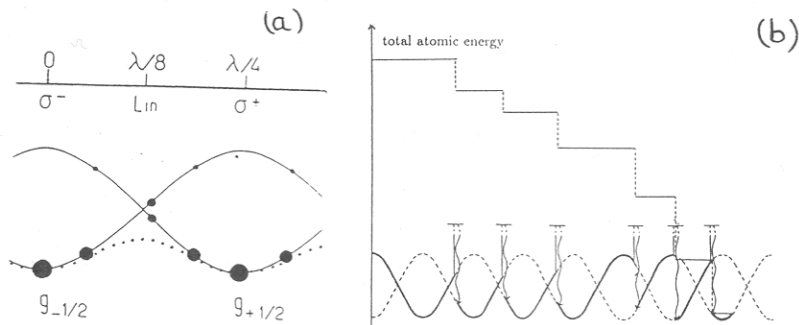


Fig. 2a: Light shifted energies and steady-state populations for a $J_g = 1/2$ ground state and for a negative detuning. The lowest sublevel, having the largest light shift, is also the most populated one. We have plotted in broken lines the average potential $\bar{U}(z)$ seen by the atom in the jumping case (§ 4.3).

Fig. 2b: Atomic Sisyphus effect. Because of the spatial modulation of the transition rates γ_{\pm} , a moving atom sees on the average more uphill parts than downhill ones and its velocity is damped. The random path sketched here has been obtained for $\delta = -5 \Gamma$ and $\Omega = 2.3 \Gamma$, and for the Cesium recoil shift $\hbar k^2/m\Gamma = 7.8 \cdot 10^{-4}$.

example of a sequence of successive discontinuous changes of the total atomic kinetic energy is represented in Fig. 2b. This constitutes an atomic realisation of the Sisyphus myth.

The intuitive limit of this type of cooling is the modulation depth U_0 of the potential: cooling is efficient until the average kinetic energy is so low that the atom cannot reach the top of the hills. (see for example the last jump represented in Fig. 2b). We will see in the following using a more rigorous treatment that the kinetic energies achievable by Sisyphus cooling are indeed on the order of a fraction of U_0 .

3. QUANTUM TREATMENT OF SISYPHUS COOLING

3.1 Principle of the Quantum Treatment

In order to make a quantitative treatment of Sisyphus cooling, we have made a numerical integration of the equation of motion of the atomic density matrix σ , involving both internal and external degrees of freedom. From the steady state value of σ , we can then derive several features of the atomic stationary distribution. For instance, the quantity:

$$\pi(p) = \sum_{\text{int}} \langle \text{int}, p | \sigma | \text{int}, p \rangle, \quad (3.1)$$

where the sum bears on all internal atomic states, gives the stationary momentum distribution. Similarly,

$$\mathcal{P}(z) = \sum_{\text{int}} \langle \text{int}, z | \sigma | \text{int}, z \rangle \quad (3.2)$$

gives the spatial repartition of the atoms, etc...

The equation of evolution of σ is [9]:

$$\dot{\sigma} = \frac{i}{\hbar}[\sigma, H] + (\dot{\sigma})_{SE} \quad (3.3)$$

where the total hamiltonian H involves the center of mass kinetic energy term $P^2/2m$, the atomic internal Hamiltonian H_{int} and the atom laser coupling V_{AL} :

$$H_{int} = \sum_{m_e=-3/2}^{3/2} \hbar\omega_A |J_e, m_e\rangle \langle J_e, m_e| \quad (3.4a)$$

$$V_{AL} = \frac{\hbar\Omega}{i\sqrt{2}} \sin kZ \left(|e_{3/2}\rangle \langle g_{1/2}| + \frac{1}{\sqrt{3}} |e_{1/2}\rangle \langle g_{-1/2}| \right) e^{-i\omega_L t} + h.c. \\ + \frac{\hbar\Omega}{\sqrt{2}} \cos kZ \left(|e_{-3/2}\rangle \langle g_{-1/2}| + \frac{1}{\sqrt{3}} |e_{-1/2}\rangle \langle g_{1/2}| \right) e^{-i\omega_L t} + h.c. \quad (3.4b)$$

where Z represents the atomic center of mass position operator. The term $(\dot{\sigma})_{SE}$ describes the relaxation of σ due to spontaneous emission processes.

To solve the equation of evolution (3.3), we expand σ in the momentum basis and we look for the evolution of matrix elements of the type $\langle i, p|\sigma|i', p'\rangle$, where i and i' stand for two internal states of the atom, and p and p' for two momenta. We get for instance:

$$\dot{\sigma}(g_{1/2}, p; e_{3/2}, p') = - \left(i \left(\delta + \frac{p^2 - p'^2}{2m\hbar} \right) + \frac{\Gamma}{2} \right) \sigma(g_{1/2}, p; e_{3/2}, p') \\ + \frac{i\Omega}{2\sqrt{2}} \left(\langle g_{1/2}, p|\sigma|g_{1/2}, p' + \hbar k \rangle - \langle g_{1/2}, p|\sigma|g_{1/2}, p' - \hbar k \rangle \right) \\ + \frac{i\Omega}{2\sqrt{2}} \left(\langle e_{3/2}, p + \hbar k|\sigma|e_{3/2}, p' \rangle - \langle e_{3/2}, p - \hbar k|\sigma|e_{3/2}, p' \rangle \right) \\ - \frac{i\Omega}{2\sqrt{6}} \left(\langle e_{-1/2}, p + \hbar k|\sigma|e_{3/2}, p' \rangle + \langle e_{-1/2}, p - \hbar k|\sigma|e_{3/2}, p' \rangle \right), \quad (3.5)$$

where we have put:

$$\sigma(g_{1/2}, p; e_{3/2}, p') = \langle g_{1/2}, p|\sigma|e_{3/2}, p' \rangle \exp(-i\omega_L t) \quad (3.6)$$

and where we have used:

$$e^{\pm ikZ}|p\rangle = |p \pm \hbar k\rangle. \quad (3.7)$$

In order to minimize the number of matrix elements involved in the calculation, we have chosen to discretize the momenta on a grid with the largest step compatible with equations such as (3.5). Thus we have chosen

$$\text{for } g_{1/2}, e_{1/2}, e_{-3/2}, \quad p = -\frac{\hbar k}{2} + 2n\hbar k \\ \text{for } g_{-1/2}, e_{3/2}, e_{-1/2}, \quad p = \frac{\hbar k}{2} + 2n'\hbar k \quad (3.8)$$

where n and n' are positive or negative integers, and where the terms $\pm\hbar k/2$ have been put to keep the symmetry between $g_{+1/2}$ and $g_{-1/2}$. One can easily check that this momentum discretisation allows the integration of the evolution equation of optical "coherences" (matrix

elements involving one g and one e) such as (3.5) or of ee matrix elements (terms involving two excited states). On the other hand the evolution of ground state matrix elements (terms with two g) is more complicated because of the feeding of these terms by spontaneous emission. For instance, one gets [9]:

$$\begin{aligned} \langle (g_{1/2}, p | \sigma | g_{1/2}, p') \rangle_{S.E.} = & \Gamma \int dp'' \mathcal{N}_{\sigma_+}(p'') \langle e_{3/2}, p + p'' | \sigma | e_{3/2}, p' + p'' \rangle \\ & + \frac{2\Gamma}{3} \int dp'' \mathcal{N}_{\pi}(p'') \langle e_{1/2}, p + p'' | \sigma | e_{1/2}, p' + p'' \rangle \\ & + \frac{\Gamma}{3} \int dp'' \mathcal{N}_{\sigma_-}(p'') \langle e_{-1/2}, p + p'' | \sigma | e_{-1/2}, p' + p'' \rangle \end{aligned} \quad (3.9)$$

where $\mathcal{N}_{\epsilon}(p'')dp''$ is the probability that, when a fluorescence photon with ϵ polarization is emitted, it will have a momentum along z between p'' and $p'' + dp''$ (dipole radiation pattern). Since p'' varies between $-\hbar k$ and $+\hbar k$, the only way to make (3.9) consistent with the momentum discretization is to take :

$$\begin{aligned} \mathcal{N}_{\sigma_+}(p'') = \mathcal{N}_{\sigma_-}(p'') = & \frac{1}{2}(\delta(p'' - \hbar k) + \delta(p'' + \hbar k)) \\ \mathcal{N}_{\pi}(p'') = & \delta(p''). \end{aligned} \quad (3.10)$$

This means that we will consider in the following that σ_{\pm} fluorescence photons are emitted along the Oz axis, while π polarized fluorescence photons are emitted orthogonally to the z axis. This constitutes a simplification of the real atomic dipole radiation pattern, but the modifications induced on the final calculated atomic distribution are small.

Once this approximation is made, we are left with a set of coupled differential equations that we truncate at a large value p_{max} of p and p' (p_{max} ranges between $40 \hbar k$ and $100 \hbar k$). We can numerically integrate these equations until the density matrix elements reach their steady state values, which are checked to be independent of the truncation p_{max} . Three independent parameters are necessary to specify the steady state : the reduced Rabi frequency Ω/Γ , the reduced detuning δ/Γ and the reduced recoil shift $\hbar k^2/m\Gamma$. Before giving the results of this integration, we now indicate how these equations can be simplified in the low intensity limit which is of interest here.

3.2 The Low Intensity Approximation

The previous equations such as (3.5) contain all the physics of the motion of a $J_g = 1/2 \longleftrightarrow J_e = 3/2$ atom in a lin \perp lin configuration. They are valid for any laser intensity and detuning, provided that the error introduced by the truncation on p is small. In particular they can describe saturation effects, if s_0 becomes of the order or larger than 1, and also Doppler cooling when the momenta p are such that kp/m is not negligible compared to Γ .

Since we are dealing here mainly with low intensity situations, we can simplify these equations of motion which makes the numerical resolution much faster. The approximation consists in neglecting excited state matrix elements in comparison with ground state matrix elements. This allows a direct calculation of optical coherences and excited state coherences and populations only in terms of ground state matrix elements. Eq. 3.5 gives for instance in steady state:

$$\begin{aligned} \sigma(g_{1/2}, p; e_{3/2}, p') = & \frac{i\Omega/2\sqrt{2}}{i(\delta + (p^2 - p'^2)/2m\hbar) + \Gamma/2} (\langle g_{1/2}, p | \sigma | g_{1/2}, p' + \hbar k \rangle \\ & - \langle g_{1/2}, p | \sigma | g_{1/2}, p' - \hbar k \rangle). \end{aligned} \quad (3.11)$$

We then replace these expressions for eg , ge and ee matrix elements in the equation of evolution of the ground state matrix elements so that we are left with equations involving only terms such as $\langle g_{\pm 1/2}, p | \sigma | g_{\pm 1/2}, p' \rangle$. This constitutes a considerable simplification of the initial numerical problem.

A second simplifying approximation consists in neglecting the kinetic energy term $(p^2 - p'^2)/2m\hbar$ appearing in the denominator of (3.11). Indeed this term can be written $[(p + p')/m][(p - p')/\hbar]$ where $(p + p')/m$ is a typical atomic velocity \bar{v} , while $(p - p')/\hbar$ is the inverse of the characteristic length of the spatial distribution, i.e. k (this will be made more clear in the Wigner representation in § 4). This approximation therefore amounts to neglecting the Doppler shift $k\bar{v}$ in comparison with Γ .

Note that on the contrary we do not neglect the term $(p^2 - p'^2)/2m$ in the evolution of $\langle g_{1/2}, p | \sigma | g_{1/2}, p' \rangle$, because this term has then to be compared with the feeding terms appearing in (3.9) such as $\Gamma \langle e_{3/2}, p | \sigma | e_{3/2}, p' \rangle \sim \Gamma s_0$, and we do not make any assumption on the respective sizes of $k\bar{v}$ and Γs_0 .

Once these two approximations are made, the quantum problem becomes very close to the simple model presented in § 2: all the dynamics is restricted to the ground state, and the residual Doppler cooling has been neglected so that one is left only with Sisyphus cooling.

3.3 Results of the quantum treatment

Since we have developed the two versions of the program solving the set of differential equations, either keeping all terms (§ 3.1) or restricting the set of equations with the low intensity assumption (§ 3.2), we can check whether the approximations presented above are justified. We have found that for $|\delta| \geq 3\Gamma$, and $s_0 \leq 0.1$, the results obtained by the two methods are close. For instance, for $\hbar k^2/m\Gamma = 7.8 \cdot 10^{-4}$ (corresponding to the Cesium atom recoil shift), and for $\Omega = \Gamma$, $\delta = -3\Gamma$, we get a steady state momentum distribution with $p_{r.m.s.} \simeq 7.4 \hbar k$ using the complete set of equations, and with $p_{r.m.s.} \simeq 7.7 \hbar k$ neglecting Doppler cooling and saturation effects. Consequently, we will only present in the following results obtained in the low power approach, which is much less computer-time consuming, keeping in mind that the addition of Doppler cooling could slightly reduce the width of the momentum distributions.

We have given in Fig. 3a a set of results for the momentum distribution obtained for the cesium recoil shift and for a detuning $\delta = -5\Gamma$. The Rabi frequency Ω varies between 0.1Γ and 2.0Γ . All distributions are equally normalized on the interval $[-40 \hbar k, 40 \hbar k]$. It clearly appears that there exists an optimal Rabi frequency around 0.5Γ for getting a high and narrow distribution.

To get more quantitative results, we have plotted in Fig. 3b the average kinetic energy $\bar{E}_K = (p_{r.m.s.})^2/2m$ in units of the recoil energy $E_R = \hbar^2 k^2/2m$. \bar{E}_K is calculated on a range $[-100 \hbar k, 100 \hbar k]$ for various sets of parameters δ , Ω and $\hbar k^2/2m$. For a given recoil shift and a given detuning, \bar{E}_K is remarkably linear with the laser intensity Ω^2 , provided Ω^2 is sufficiently large. When Ω^2 is decreased, \bar{E}_K reaches a minimum value and then increases again as Ω^2 tends to zero.

Data of Fig. 3b also clearly show that, for large δ , \bar{E}_K/E_R is actually a function of a single parameter, $m\Omega^2/|\delta|\hbar k^2$, which is proportionnal to U_0/E_R . The minimal value of \bar{E}_K is obtained for:

$$U_0 \simeq 105 E_R \quad (3.12)$$

and is found to be:

$$(E_K)_{\min} \simeq 40 E_R \rightarrow (p_{r.m.s.})_{\min} \simeq 6.3 \hbar k. \quad (3.13)$$

One can see from Fig. 3b that $U_0 \simeq 100 E_R$ appears as a threshold potential for having good Sisyphus cooling: below this value, the steady-state kinetic energy increases very rapidly as U_0 decreases.

Now, one might ask whether these momentum distributions are Gaussian and can be assigned a temperature. In Fig. 4, we have plotted, for $\delta = -15\Gamma$, both $p_{r.m.s.}$ and $\delta p_{1/\sqrt{e}}$ (half width of the distribution at $1/\sqrt{e}$ of full height) vs Ω/Γ . For a Gaussian distribution, these two quantities are equal. Here, one clearly sees that a discrepancy appears either for very low or high Rabi frequencies. In both cases, $p_{r.m.s.}$ is larger than $\delta p_{1/\sqrt{e}}$, indicating the presence of large wings in the momentum distributions. The minimal value reached by $\delta p_{1/\sqrt{e}}$ is only:

$$(\delta p_{1/\sqrt{e}})_{\min} \simeq 3 \hbar k \quad (3.14)$$

and is obtained for:

$$U_0 \simeq 25 E_R. \quad (3.15)$$

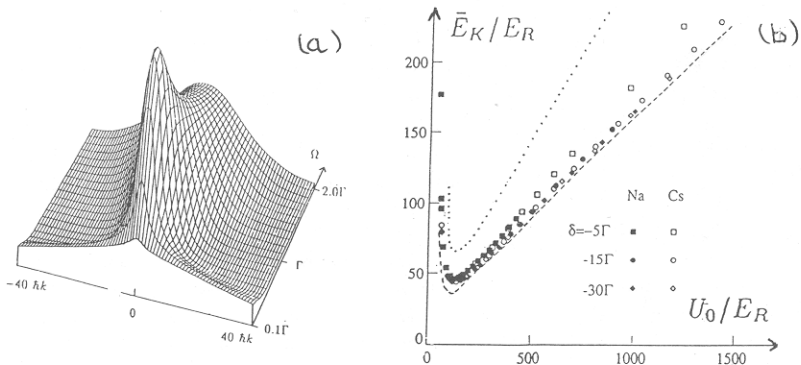


Fig. 3a: Steady-state momentum distributions obtained for a detuning $\delta = -5\Gamma$ for various Rabi frequencies Ω .

Fig. 3b: Average kinetic energy \bar{E}_K in units of the recoil energy E_R versus U_0/E_R . The results of the semi-classical treatment (§ 4) are indicated in dotted lines (spatial modulation neglected) and in broken lines (spatial modulation included for the case of "oscillating particles").

Finally, we have looked for the spatial atomic distribution $\mathcal{P}(z)$. This distribution is modulated in z with a period $\lambda/4$. The distribution is found to be nearly uniform for small U_0 ($U_0 \leq 100 E_R$); the atoms are on the contrary localized around the points $z = n\lambda/4$ for large U_0 .

To summarize the results of this quantum treatment, we have shown that, for large detunings, the steady state momentum distributions obtained by Sisyphus cooling depend only on a single parameter U_0/E_R when $\hbar k$ is chosen as the momentum unit. This has to be compared

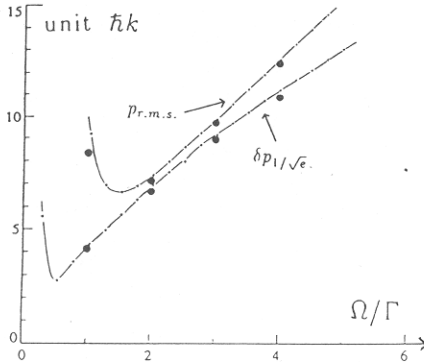


Fig. 4: Comparison between the r.m.s. momentum $p_{r.m.s.}$ and the width at $1/\sqrt{e}$ of the steady-state momentum distribution, for the cesium recoil shift and for a detuning of -15Γ . These two quantities would be equal in the case of a Gaussian momentum distribution. The dots indicate the results of a Monte-Carlo treatment (see § 4).

with the result for Doppler cooling where the momentum distributions are Gaussian with a temperature (in units of $\hbar\Gamma/k_B$) depending only on δ/Γ . Here the situation is more complex since the momentum distributions are not always Gaussian. Therefore they cannot be characterized by a single number such as a temperature. Depending whether one looks for a “compact” momentum distribution (small $p_{r.m.s.}$) or a very narrow central peak (small $\delta p_1/\sqrt{e}$), the optimal value for the “universal parameter” U_0/E_R changes by a numerical factor of the order of 4.

3.4 Physical discussion

We now compare the results of this quantum approach with the ones obtained from a simple analytical treatment [7]. That treatment was limited to a situation where the cooling could be described, after a spatial averaging, by a force linear with the atomic momentum p and a diffusion coefficient independent of p . It led to Gaussian momentum distributions with an average kinetic energy given by $\bar{E}_K = 3U_0/16$.

Here we recover this linear dependence of \bar{E}_K vs U_0 over a wide range of parameters. The slope ($\partial\bar{E}_K/\partial U_0$) is 0.14 instead of $3/16 \simeq 0.19$, which is in remarkable agreement if one takes into account all the approximations introduced in the analytical treatment of [7].

There is however a discrepancy between the results obtained here and the predictions of [7]. It indeed appears from the results of this full quantum treatment that Sisyphus cooling works better than what was expected! In [7], Sisyphus cooling was expected to be efficient as long as the cooling force was linear with p over all the steady-state momentum distribution which has a typical width $p_{r.m.s.}$. This requirement led to a minimum kinetic energy given by:

$$\bar{E}_K \gg E_R \frac{\delta^2}{\Gamma^2}. \quad (3.16)$$

On the contrary, the minimal kinetic energy found here is independent of the detuning δ even for very large detunings. This will be explained further as due to the fact that Sisyphus cooling

works even if the *r.m.s.* momentum is outside the range of linearity of the force. For such large momenta, indeed, the diffusion coefficient, and therefore the heating, decrease when p increases so that Sisyphus cooling may remain efficient.

Another unexpected feature of the results of this quantum approach concerns the deviation from a Gaussian of the steady-state momentum distribution obtained for large modulation depths U_0 (Fig. 4). This deviation has to be connected to the apparition of an important modulation of the spatial atomic distribution $\mathcal{P}(z)$ in steady-state. Such a localization of the atoms had not been taken into account in [7] because of the spatial averaging of the force and of the momentum diffusion coefficient.

We now present an analytical treatment which gives a good account for these two features, minimum of \bar{E}_K vs U_0 at low U_0 , and localization of atoms for large U_0 .

4. SEMI-CLASSICAL TREATMENT OF SISYPHUS COOLING

In order to get some physical insights in the results given by the quantum treatment presented in the previous section, we now turn to an approach in which the external motion can be analyzed in classical terms. The corresponding equations of motion can be derived from an expansion in $\hbar k/\bar{p} \ll 1$ of the quantum equations of evolution. We will see that this expansion validates the physical pictures given in § 2, and that it gives an interpretation for most of the results given by the quantum treatment.

4.1 Expansion of the Equations of Motion

The principle of the calculation is very similar to the one developed for a 2-level atom by various authors [10]. We start from the Wigner representation of the atomic density operator:

$$W(z, p, t) = \frac{1}{\hbar} \int dv \langle p + \frac{v}{2} | \sigma | p - \frac{v}{2} \rangle \exp\left(\frac{izv}{\hbar}\right). \quad (4.1)$$

Note that $W(z, p, t)$ is still an operator with respect to the internal degrees of freedom. For instance, (3.5) can be written:

$$\begin{aligned} \frac{\partial}{\partial t} (e^{-i\omega_L t} \langle g_{1/2} | W(z, p, t) | e_{3/2} \rangle) &= - (i\delta + \frac{\Gamma}{2} + \frac{p}{m} \frac{\partial}{\partial z}) \langle g_{1/2} | W(z, p, t) | e_{3/2} \rangle e^{-i\omega_L t} \\ &+ \frac{i\Omega}{2\sqrt{2}} e^{ikz} \langle g_{1/2} | W(z, p + \frac{\hbar k}{2}, t) | g_{1/2} \rangle \\ &- \frac{i\Omega}{2\sqrt{2}} e^{-ikz} \langle g_{1/2} | W(z, p - \frac{\hbar k}{2}, t) | g_{1/2} \rangle, \end{aligned} \quad (4.2)$$

where we have neglected, in the low intensity limit, the two last lines of (3.5) since they involve only matrix elements of W between excited states.

Now, since we have seen in § 3 that the momentum extension $p_{r.m.s.}$ of the steady state remains larger than $\hbar k$, we can expand W in the following way :

$$W(z, p + \hbar k) \simeq W(z, p) + \hbar k \frac{\partial W}{\partial p}(z, p) + \dots$$

We note that the atomic kinetic energy contribution, leading to the free flight term $p/m \cdot \partial W / \partial z$, is easy to evaluate in the Wigner representation since $\partial W / \partial z$ is of the order of kW . In expressions such as (4.2), this contribution is therefore negligible if $kp/m \ll \Gamma$.

We now proceed in the same way as in § 3.3. We eliminate optical coherences and excited state populations and coherences to get two equations dealing only with:

$$w_{\pm}(z, p, t) = \langle g_{\pm 1/2} | W(z, p, t) | g_{\pm 1/2} \rangle . \quad (4.3)$$

After some algebra we obtain:

$$\left(\frac{\partial}{\partial t} + \frac{p}{m} \frac{\partial}{\partial z} - \frac{dU_{\pm}}{dz} \frac{\partial}{\partial p} \right) w_{\pm} = \mp (\gamma_{+}(z) w_{+} - \gamma_{-}(z) w_{-}) + \frac{\hbar^2 k^2 \Gamma s_0}{18} \frac{\partial^2}{\partial p^2} ((10 - \cos 2kz) w_{\pm} + w_{\mp}) \quad (4.4)$$

This equation is a straightforward validation of the physical picture given in § 2. It describes the motion of a particle with mass m , moving on the bi-potential $U_{\pm}(z)$ given in (2.4), with random jumps between the levels $g_{\pm 1/2}$ with rates $\gamma_{\pm}(z)$ (Eqs. 2.8,9). The second line in (4.4) corresponds to the atomic momentum diffusion in absorption and emission processes due to the discreteness of the photon momentum. For instance the atom on level $g_{1/2}$ can jump to $e_{3/2}$ or $e_{-1/2}$ by absorbing a laser photon, and come back to $g_{1/2}$ by emitting a fluorescence photon. The ground state sublevel is not changed in such a process but there is a momentum diffusion due to the randomness of the momentum ($\pm \hbar k$) of both the absorbed laser photon and the emitted fluorescence one. We note that the momentum diffusion coefficient appearing in (4.4) has the same order of magnitude ($\hbar^2 k^2 \Gamma s_0$) as the one found for a two level atom in a weak standing wave.

The last term of the second line of (4.4) describes a diffusive coupling between w_{+} and w_{-} . It does not vanish for the values of z for which $\gamma_{+}(z)$ and $\gamma_{-}(z)$ vanish, and where one would expect that no transfer is possible between $g_{-1/2}$ and $g_{1/2}$. The existence of such a term is actually due to the fact that the atomic wave packet has a finite extension $\Delta x \simeq \hbar/\Delta p$, which gives rise to correction terms for the transfer rates of the order of $(\Delta x/\lambda)^2 \simeq \hbar^2 k^2/\Delta p^2$.

4.2 The Steady-State Distribution in the Limit of Negligible Spatial Modulation

We now turn to the research of an analytical solution to the semi-classical equations of motion (4.4). We begin in this section by introducing a rather crude approximation which however gives results in good agreement with the ones obtained from the quantum approach. We look for the evolution of the atomic distribution function given by:

$$\psi(z, p, t) = w_{+}(z, p, t) + w_{-}(z, p, t) \quad (4.5)$$

and we make the very simple assumption that ψ is actually independent of z , i.e. the total atomic distribution function has a negligible spatial modulation in steady state. We will come back to this hypothesis at the end of the calculation.

Summing the two equations (4.4) for w_{+} and w_{-} , we get in steady state:

$$\frac{p}{m} \frac{\partial \psi}{\partial z} = -F(z) \frac{\partial \psi}{\partial p} + D_0 \frac{\partial^2 \psi}{\partial p^2} \quad (4.6a)$$

with:

$$\frac{\partial \psi}{\partial z} \simeq 0 \quad (4.6b)$$

$$F(z) = -\frac{dU_{+}}{dz} = \frac{dU_{-}}{dz} = kU_0 \sin 2kz \quad (4.6c)$$

$$\varphi(z, p, t) = w_{+}(z, p, t) - w_{-}(z, p, t) \quad (4.6d)$$

$$D_0 = 11\hbar^2 k^2 \Gamma s_0 / 18 . \quad (4.6e)$$

Note that we have neglected the modulation in $\cos 2kz$ of the momentum diffusion coefficient appearing in (4.4).

Now the evolution of the difference φ between w_+ and w_- is obtained also from (4.4):

$$\left(\frac{\partial}{\partial t} + \frac{p}{m} \frac{\partial}{\partial z}\right) \varphi = -F \frac{\partial \psi}{\partial p} + (\gamma_- - \gamma_+) \psi - (\gamma_+ + \gamma_-) \varphi + \frac{1}{2} \hbar^2 k^2 \Gamma s_0 \frac{\partial^2 \varphi}{\partial p^2}. \quad (4.7)$$

The last term of (4.7) is small compared to $(\gamma_+ + \gamma_-) \varphi = (2\Gamma s_0/9) \varphi$ since $\bar{p} \gg \hbar k$ and will be neglected in the following. In steady state, (4.7) can then be integrated to give for $p > 0$:

$$\varphi(z, p) = \frac{m}{p} \int_{-\infty}^z dz' e^{-2kp_c(z-z')/p} \left((\gamma_- - \gamma_+)(z') \psi - F(z') \frac{\partial \psi}{\partial p} \right) \quad (4.8a)$$

with:

$$\frac{kp_c}{m} = \frac{\Gamma s_0}{9}. \quad (4.8b)$$

Replacing γ_{\pm} and F by their expression (2.8-9 and 4.6c) and with the assumption that ψ is independent of z , we get :

$$\varphi(z, p) = \frac{-p/p_c}{1 + (p/p_c)^2} \left[\left(\sin 2kz + \frac{p_c}{p} \cos 2kz \right) \psi - \frac{mU_0}{2p_c} \left(\cos 2kz - \frac{p_c}{p} \sin 2kz \right) \frac{\partial \psi}{\partial p} \right]. \quad (4.9)$$

We now put this expression for φ in (4.6a) and we average the result over a wavelength, in order to be consistent with the assumption that ψ is not modulated in steady state. This gives:

$$0 = \frac{\partial}{\partial p} \left(\left(\frac{\alpha p/m}{1 + (p/p_c)^2} \right) \psi + \left(\frac{D_1}{1 + (p/p_c)^2} + D_0 \right) \frac{\partial \psi}{\partial p} \right) \quad (4.10)$$

with:

$$\alpha = \frac{kU_0}{2p_c} = -3\hbar k^2 \frac{\delta}{\Gamma} \quad (4.11a)$$

$$D_1 = \frac{kmU_0^2}{4p_c} = \hbar^2 k^2 \Gamma s_0 \frac{\delta^2}{\Gamma^2} \quad (4.11b)$$

Expression (4.10) has a straightforward interpretation: in steady state, the momentum distribution results from an equilibrium between a cooling force due to the Sisyphus effect:

$$f(p) = -\frac{\alpha p/m}{1 + (p/p_c)^2} \quad (4.12)$$

and heating due to momentum diffusion described by the diffusion coefficient:

$$D(p) = \frac{D_1}{1 + (p/p_c)^2} + D_0. \quad (4.13)$$

The expression (4.12) for the cooling force has already been derived elsewhere [7]. It is equal to the average of the two state dependent forces $-(dU_{\pm}/dz)$, weighted by the steady state populations of these states for an atom moving with velocity $v = p/m$.

The momentum diffusion (4.13) has two contributions. The term D_0 has been discussed above; it corresponds to the fluctuations of the momentum carried away by the fluorescence photons and to the fluctuations in the difference between the number of photons absorbed in

each of the two laser waves. The term proportional to D_1 corresponds to the fluctuations of the instantaneous gradient force $F_g(t)$ oscillating back and forth between $-dU_+/dz$ and $-dU_-/dz$ at a rate $1/\tau_P$. It is approximatively equal to the time integral of the correlation function of $F_g(t)$:

$$I(p) = \int_0^\infty \langle F_g(t-\tau)F_g(t) \rangle_{\text{position}} d\tau$$

$$= \frac{D_1}{1+(p/p_c)^2} \left(1 - \frac{5/4}{1+(p/p_c)^2} + \frac{1}{(1+(p/p_c)^2)^2} \right)$$

which gives a good understanding of the variation with p of this diffusion term: if the atom moves slowly ($p \ll p_c$) it travels over a small fraction of a wavelength during the correlation time τ_P . Then there is a strong correlation between $F_g(t-\tau)$ and $F_g(t)$ and I is large. On the other hand, if $p \gg p_c$, the atom travels over many wavelengths before changing level and the value of I is decreased since the correlation between $F_g(t-\tau)$ and $F_g(t)$ becomes small.

Remark: many terms have been left out in the procedure which led to (4.10) and it is possible to get a more accurate (but more complicated) equation for ψ if one keeps some of these terms. For instance, for $p = 0$, there is a discrepancy by a factor 4/3 between the momentum diffusion coefficient $D(p)$ found here and the value of $I(p)$. This discrepancy can be lifted if one takes into account more spatial harmonics in the derivation of the Fokker-Planck equation (4.10).

We now look for the solution of (4.10). This solution can be written:

$$\psi(p) = \psi(0) \exp \left(\int_0^p \frac{f(p')}{D(p')} dp' \right) \quad (4.14)$$

We first note that, if D_0 is neglected, this momentum distribution is Gaussian with $k_B T = D_1/\alpha = U_0/2$, since f/D is linear in p . Therefore we see that Sisyphus cooling may lead to narrow momentum distributions even if the cooling force is not linear in p over the steady-state momentum distribution. This is due to the fact that the momentum diffusion associated with the Sisyphus mechanism actually decreases faster (in $1/p^2$) than the cooling force (in $1/p$). We therefore understand in this way why the real lower bound on \bar{E}_K is actually smaller than the one given in (3.16).

We now take into account D_0 : We then get :

$$\psi(p) = \frac{\psi(0)}{(1+p^2/\bar{p}_c^2)^A} \quad (4.15)$$

with :

$$\bar{p}_c = p_c \sqrt{1 + D_1/D_0} \Rightarrow \frac{\bar{p}_c}{\hbar k} \approx \frac{1}{\sqrt{88}} \frac{U_0}{E_R} \quad \text{for } |\delta| \gg \Gamma \quad (4.16a)$$

$$A = \frac{\alpha p_c^2}{2mD_0} = \frac{U_0}{44 E_R} \quad (4.16b)$$

Expression (4.15) exhibits several features similar to the ones derived from the quantum treatment. First we see from (4.16a,b) that, if we express p in units of $\hbar k$, the steady-state distribution depends only on U_0/E_R . One finds for the r.m.s. momentum after some algebra:

$$\bar{E}_K = \frac{1}{4} \frac{U_0^2}{U_0 - 66 E_R} \quad \text{for } U_0 > 66 E_R, \quad (4.17)$$

the integral giving $\langle p^2 \rangle$ diverging for $U_0 \leq 66 E_R$. The variations of \bar{E}_K as a function of U_0 have been plotted in dotted lines in Fig. 3b. They are in good qualitative agreement with the quantum results for small values (< 100) of U_0/E_R . As U_0/E_R increases, a discrepancy between the two results appears. This is due to the fact, for large U_0 , the particles become localized in the potential valleys (Fig. 4b), and the hypothesis that ψ is not spatially modulated becomes very unrealistic.

We also note that for $U_0 \leq 22 E_R$, Eq. 4.15 leads to a non normalisable distribution ($A \leq 0.5$), which means that the Sisyphus cooling is then too weak to maintain the particles around $p = 0$ in steady state.

To summarize, one should consider this analytical approach as a good qualitative treatment, valid mainly around and below the minima of the average kinetic energy plotted in Fig. 3b. On the other hand, much above these minima, *i.e.* for large U_0/E_R , this treatment predicts that \bar{E}_K becomes on the order of $U_0/4$. With such a kinetic energy, much smaller than the potential depth U_0 , the hypothesis of non localised particles which is at the basis of this treatment is very unrealistic. We therefore present now some elements concerning this regime where the particles get localized.

4.3 Taking into Account the Localization

An important parameter for characterizing the motion of trapped particles is the ratio between the harmonic oscillation frequency of the particles in the wells:

$$\Omega_{\text{osc}} = \sqrt{\frac{4\hbar|\delta|s_0k^2}{3m}} \quad (4.18)$$

and the rate $1/\tau_P$ at which the particles jump from one level (g_{\pm}) to the other one (g_{\mp}). This ratio is:

$$\Omega_{\text{osc}}\tau_P = \sqrt{27 \frac{\hbar k^2 |\delta|}{m s_0 \Gamma^2}} = \sqrt{36 \frac{E_R \delta^2}{U_0 \Gamma^2}} \quad (4.19a)$$

$$= \sqrt{\frac{U_0}{2p_c^2/m}} \quad (4.19b)$$

If $\Omega_{\text{osc}}\tau_P \gg 1$, we are in a situation where the particles make several oscillations before changing level. On the other hand, if $\Omega_{\text{osc}}\tau_P \ll 1$, the particles can make several transitions between $g_{1/2}$ and $g_{-1/2}$ in a single oscillation period. These two regimes have been represented in Fig. 5 as a function of $|\delta|/\Gamma$ and Ω/Γ , for the cesium recoil shift.

In order to show more clearly the relevance of this parameter $\Omega_{\text{osc}}\tau_P$, it is worthwhile to rewrite (4.4) in terms of a reduced set of parameters:

$$x = kz \quad (4.20a)$$

$$u = p/\sqrt{2mU_0} \quad (4.20b)$$

In steady state this leads to:

$$u \frac{\partial w_{\pm}}{\partial x} \pm \frac{1}{2} \sin 2x \frac{\partial w_{\pm}}{\partial u} = \frac{1}{\Omega_{\text{osc}}\tau_P} \left(\mp (w_{+} \cos^2 x - w_{-} \sin^2 x) + \frac{E_R}{4U_0} \frac{\partial^2}{\partial u^2} ((10 - \cos 2x)w_{\pm} + w_{\mp}) \right) \quad (4.21)$$

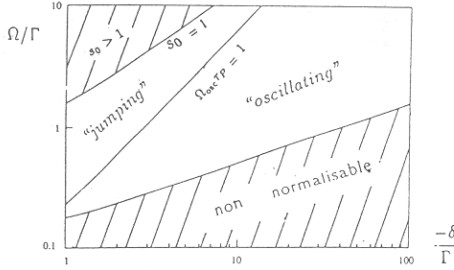


Fig. 5: Various regimes for the motion of an atom (with the cesium recoil shift) in the $\text{lin}\perp\text{lin}$ configuration. Depending on the value of the detuning and the Rabi frequency, the atom is either in the “oscillating” case or in the “jumping” one.

We now present for each of these regimes an analytical approach based on an expansion of this equation in powers of the small parameter $\Omega_{osc}\tau_P$ (jumping situation) or $(\Omega_{osc}\tau_P)^{-1}$ (oscillating situation). Here, emphasis is put mainly on the derivation of equations of motion. A detailed analysis of the solution of these equations and of the corresponding results for the position, momentum, energy... distributions will be presented in a subsequent paper.

4.3.a The case of jumping particles: $\Omega_{osc}\tau_P \ll 1$

We first note from (4.19a) that, in this domain, the potential U_0 is much larger than $36 E_R$ (for $|\delta| \geq \Gamma$) so that we are in the linear domain of variation of \bar{E}_K with U_0 (Fig. 3b). On the other hand, (4.19b) implies that U_0 is much smaller than $p_c^2/2m$, so that $\hbar k \ll p_{rms} \ll p_c$. We are therefore in the domain where the cooling force is linear with p , and where the diffusion coefficient is independant of p . We now show that it is possible in this case to derive a Fokker-Planck equation for $\psi(z, p, t)$. Note that the condition $\Omega_{osc}\tau_P \ll 1$ can also be written as $T_{int} \ll T_{ext}$, since the optical pumping time τ_P can be considered as a characteristic internal time T_{int} , whereas the oscillation period $2\pi/\Omega_{osc}$ in a potential well is a typical external time T_{ext} . It is then well known that such a separation of time scales allows one to eliminate adiabatically the fast variables and to derive a Fokker-Planck equation for the slow variable $\psi(z, p, t)$.

Starting from (4-8), in which we keep the spatial modulation of ψ , we get at the lowest order in $\hbar k/p$:

$$\varphi(z, p) = -\cos 2kz \psi(z, p) \quad (4.22)$$

Indeed the kernel $\exp(-2kp_c(z-z')/p)$ is nearly equal to $\delta(z-z')p/2kp_c$, since $|p| \ll p_c$. Note that (4.22) can be rewritten as $w_+(z, p) = \sin^2 kz \psi(z, p)$ and $w_-(z, p) = \cos^2 kz \psi(z, p)$, which corresponds to the internal stationary state of an atom at rest in z and which gives the solution of (4.21) at order 0 in $\Omega_{osc}\tau_P$ and for $U_0 \gg E_R$. We now insert (4.22) in the equation of evolution of ψ (4.6a) which gives still at lowest order:

$$\frac{p}{m} \frac{\partial \psi}{\partial z} = F(z) \cos 2kz \frac{\partial \psi}{\partial p}. \quad (4.23)$$

At this order, the particles move in an average potential $\bar{U}(z)$, plotted in dotted lines in Fig.2a, and given by [7]:

$$\bar{U}(z) = \frac{U_0}{4} \sin^2(2kz). \quad (4.24)$$

At the next order we get after some calculation and using (4.23):

$$\begin{aligned}\varphi(z, p) &= - \left(\cos 2kz + \frac{p}{p_c} \sin 2kz \right) \psi(z, p) + \frac{p}{2kp_c} \cos 2kz \frac{\partial \psi}{\partial z} - \frac{m}{2kp_c} F(z) \frac{\partial \psi}{\partial p} \\ &\simeq - \left(\cos 2kz + \frac{p}{p_c} \sin 2kz \right) \psi(z, p) - \frac{m}{2kp_c} F(z) (1 - \cos^2 2kz) \frac{\partial \psi}{\partial p}\end{aligned}\quad (4.25)$$

which gives when inserted in (4-6a):

$$\frac{p}{m} \frac{\partial \psi}{\partial z} = \frac{\partial}{\partial p} \left(\left(\frac{d\bar{U}}{dz} + \frac{\bar{\alpha}(z)p}{m} \right) \psi \right) + (\bar{D}_1(z) + D_0) \frac{\partial^2 \psi}{\partial p^2} \quad (4.26)$$

with :

$$\bar{\alpha}(z) = 6\hbar k^2 \left(\frac{-\delta}{\Gamma} \right) \sin^2 2kz \quad (4.27a)$$

$$\bar{D}_1(z) = 2\hbar^2 k^2 \frac{\delta^2}{\Gamma} s_0 \sin^4 2kz \quad (4.27b)$$

This equation describes the Brownian motion of a particle in a potential $\bar{U}(z)$, with a linear friction force $-\bar{\alpha}(z)p/m$, and with a spatially varying diffusion coefficient $\bar{D}_1(z) + D_0$. We recover here the results already obtained in [7] from the usual theory of radiative forces in the limit of well separated time scales ($T_{int} \ll T_{ext}$). We can note that the oscillation frequency $\bar{\Omega}_{osc}$ in $\bar{U}(z)$:

$$\bar{\Omega}_{osc} = \sqrt{\frac{2k^2 U_0}{m}} \quad (4.28)$$

is always larger than $\bar{\alpha}(z)/m$:

$$\frac{\bar{\alpha}(z)}{m\bar{\Omega}_{osc}} = \sqrt{36 \frac{E_R}{U_0} \frac{\delta^2}{\Gamma^2} \sin^2 2kz} \leq \Omega_{osc} \tau_P \ll 1 \quad (\text{for jumping particles}). \quad (4.29)$$

This means that the motion in the average potential $\bar{U}(z)$ is underdamped so that Eq. 4.26 could now be solved by successive approximations if one parametrizes the motion with z and $\bar{E} = \bar{U}(z) + p^2/2m$, instead of z and p [11].

4.3.b The case of oscillating particles: $\Omega_{osc} \tau_P \gg 1$

We suppose now that the particles make several oscillations in a potential well before being optically pumped into another sublevel. The characteristic time for z and p , Ω_{osc}^{-1} , is then shorter than $T_{int} = \tau_P$. There is however another external variable which varies slowly, the total energy $E = U_{\pm} + p^2/2m$. We therefore parametrize the motion with the new variables z and E instead of z, p . Using:

$$\frac{p}{m} \left(\frac{\partial}{\partial z} \right)_p + F(z) \left(\frac{\partial}{\partial p} \right)_z = v \left(\frac{\partial}{\partial z} \right)_E$$

where v stands for $\sqrt{2(E - U_{\pm}(z))/m}$, we get at order zero in $(\Omega_{osc} \tau_P)^{-1}$:

$$\left(\frac{\partial w_+^{(0)}}{\partial z} \right)_E = 0 \quad (4.30)$$

which gives:

$$w_+^{(0)}(z, p) = \Phi(E) . \quad (4.31a)$$

In the same way, we obtain by symmetry:

$$w_-^{(0)}(z, p) = \Phi(E - U_+(z) + U_-(z)) . \quad (4.31b)$$

We now write (4.4) or (4.21) at order one in $(\Omega_{\text{osc}}\tau_P)^{-1}$:

$$v \left(\frac{\partial w_+^{(1)}}{\partial z} \right)_E = -\gamma_+(z)w_+^{(0)} + \gamma_-(z)w_-^{(0)} + \frac{\hbar^2 k^2 \Gamma s_0}{18} v \frac{\partial}{\partial E} \left(v \frac{\partial}{\partial E} \left((10 - \cos 2kz)w_+^{(0)} + w_-^{(0)} \right) \right) , \quad (4.32)$$

We now divide this equation by v and integrate over an oscillation period for $E < U_0$:

$$0 = - \oint \frac{dz}{v} \gamma_+(z) \Phi(E) + \oint \frac{dz}{v} \gamma_-(z) \Phi(E - U_+(z) + U_-(z)) + \frac{\hbar^2 k^2 \Gamma s_0}{18} \frac{\partial}{\partial E} \left(\oint dz v \left((10 - \cos 2kz) \Phi'(E) + \Phi'(E - U_+(z) + U_-(z)) \right) \right) . \quad (4.33)$$

For $E > U_0$, a similar equation holds, where the integral is now taken over a spatial period. Eq. 4.33 has a clear physical meaning: The first line just expresses that the rate at which particles with energy E leave level $g_{1/2}$ to $g_{-1/2}$ is equal to the rate at which particles arrive from $g_{-1/2}$ to $g_{1/2}$ with the same energy E . The second line of (4.33) corresponds to the correction to this balance due to the heating leaving the particles on the same level. For $U_0 \gg E_R$, this heating is for most energies E negligible. However it should be kept to prevent particles to accumulate in the bottom of the well U_+ (resp. U_-), where the departure rate γ_+ (resp. γ_-) vanishes. It is indeed easy to show that without this term the solution of (4.33) would diverge as $1/E$ around $E = 0$, and would therefore not be normalisable.

We have performed a numerical integration of this equation whose result is plotted in broken lines in Fig. 3b. One immediately sees that it reproduces in a very satisfactory way the results of the quantum approach in the limit of large detunings and for a given U_0 , *i.e.* in the limit $\Omega_{\text{osc}}\tau_P \gg 1$.

To summarize, we have been able in both situations (jumping or oscillating) to obtain a single equation for $\psi(z, p)$ or $\Phi(E)$. The regime of jumping particles can be treated with concepts usual in laser cooling theory: a force deriving from a potential plus a cooling force linear with the atomic momentum, and a momentum diffusion coefficient independent of p . It should be emphasized however that the range of parameters (detuning, Rabi frequency) leading to this regime is rather small (see Fig. 5). In particular, the perturbative treatment used here is valid only if $s_0 \ll 1$ and this condition, for large detunings, immediately leads to the oscillating situation rather than to the jumping one.

The theoretical study of the oscillating regime is very different from the jumping one. The equation (4.33) for $\Phi(E)$, probability for finding an atom with energy E on level $g_{1/2}$ is *not* a differential equation, contrarily to what is usually found in laser cooling. This is due to the non-locality of the atom dynamics: as the atom jumps from level $g_{1/2}$ to level $g_{-1/2}$, its energy changes suddenly from $U_+(z) + p^2/2m$ to $U_-(z) + p^2/2m$. Since $p^2/2m$ is of the order of U_0 , this

change cannot be treated as a small variation, which prevents deriving a Fokker-Planck type equation for $\Phi(E)$.

4.4 Monte-Carlo Approach

Finally, an alternative approach consists in performing a Monte-Carlo simulation of this problem. Such a simulation is made possible because no coherence appears between levels $g_{\pm 1/2}$, contrarily to what would occur for a more complex atomic transition. Furthermore, in order to be able to associate to (4.4) a classical stochastic process describable by a Monte-Carlo simulation, we have chosen to slightly simplify the second line of (4.4) by taking as a diffusion term $D_0 \partial^2 w_{\pm} / \partial p^2$.

This approach is then directly connected with the physical picture presented in § 2. It consists in a numerical integration of the equation of motion of the particles on the bi-potential $U_{\pm}(z)$, with random jumps from one potential to the other one, and also a random heating corresponding to the simplified diffusion term described just above. We record for given interaction times the position and the momentum of the particle. The steady state distributions are found to be in very good agreement with the results of the quantum treatment (see Fig. 4).

A first advantage of this Monte-Carlo method lies in the fact that it can be run on a small computer. Also it can be generalized, for the $J_g = 1/2 \longleftrightarrow J_e = 3/2$ transition, to the case of 2 or 3 dimensional Sisyphus cooling, provided that the laser configuration is such that the light polarization is always a linear combination of σ_+ and σ_- polarizations with no π component. In these conditions indeed, no coherence is built between $g_{1/2}$ and $g_{-1/2}$ and the simple picture of a particle moving on a bi-potential can be applied.

CONCLUSION

To summarize, we have presented here both a full quantum and a semi-classical treatment for the 1-D cooling of a $J_g = 1/2 \longleftrightarrow J_e = 3/2$ atomic transition in a lin-lin laser configuration. The mechanism at the basis of the cooling is a Sisyphus effect in which a given atom climbs more than it goes down in its potential energy diagram. These two treatments are in good agreement concerning the minimal "temperature" achievable by this cooling mechanism (Eqs. 3.12-15).

We have also shown that, for light shifted energies much larger than the ones minimizing the atomic kinetic energy, the atoms get localized around the minima of the potential associated with the light shifts and we have indicated the two possible approaches to this situation depending on the nature of the atomic motion around the position of these minima (see Fig. 5).

We should emphasize that there are many other schemes leading to a Sisyphus type cooling, not necessarily requiring a gradient of ellipticity of the polarization of the laser light. For instance a combination of a σ_+ standing wave and of a magnetic field can lead in 1-D to a cooling of the same type [8, 12].

In a similar way, in 2-D or 3-D, the superposition of 2 or 3 standing waves having the same phase leads to a situation where the light is linearly polarized in any point, with a rotating polarization and with a spatially varying intensity, with nodes and antinodes. As the atoms move in this configuration, a Sisyphus effect may occur for $J_g \geq 1$: it would involve a randomization of the population of the various ground-state sublevels around the nodes due to Landau-Zener type transitions, and optical pumping back into the most light shifted energy levels around the anti-nodes.

Consequently the model studied here should be considered as a particularly simple prototype of this type of cooling, but, on the other hand, the detailed algebra has probably to be readjusted for the study of any other Sisyphus type cooling mechanism.

We thank W.D. Phillips and C. Salomon for many stimulating discussions.

REFERENCES

- [1] See for example the special issue of J.O.S.A. **B6**, November 1989.
- [2] T.W. Hänsch and A. Schawlow, *Opt. Commun.* **13**, 68 (1975).
- [3] D. Wineland and W. Itano, *Phys.Rev.* **A20**, 1521 (1979).
- [4] P. Lett, R. Watts, C. Westbrook, W.D. Phillips, P. Gould and H. Metcalf, *Phys.Rev.Lett.* **61**,169 (1988).
- [5] J. Dalibard, C. Salomon, A. Aspect, E. Arimondo, R. Kaiser, N.Vansteenkiste and C. Cohen-Tannoudji, in *Proceedings of the 11th Conference on Atomic Physics*, S. Haroche, J.C. Gay and G. Grynberg, eds (World Scientific, Singapore, 1989).
- [6] S. Chu, D.S. Weiss, Y. Shevy and P.J. Ungar, in *Proceedings of the 11th Conference on Atomic Physics*, S. Haroche, J.C. Gay and G. Grynberg, eds (World Scientific, Singapore, 1989).
- [7] J. Dalibard and C. Cohen-Tannoudji, *J.O.S.A.* **B6**, 2023 (1989).
- [8] D. Weiss, P.J. Ungar and S. Chu, *J.O.S.A.* **B6**, 2072 (1989).
- [9] see e.g. Y. Castin, H. Wallis and J. Dalibard, *J.O.S.A.* **6**, 2046 (1989) and ref. in.
- [10] see e.g. J. Dalibard and C. Cohen-Tannoudji, *J.Phys.***B18**, 1661 (1985).
- [11] N.G. van Kampen, *Stochastic Processes in Physics and Chemistry*, North-Holland, 1981.
- [12] B. Sheehy, S.Q. Shang, P. van der Straten, S. Hatamian and H. Metcalf, *Phys.Rev.Lett.* **64**, 858 (1990).